

# VoroContacts: a tool for the analysis of interatomic contacts in macromolecular structures

## Supplementary information

Kliment Olechnovič and Česlovas Venclovas

Institute of Biotechnology, Life Sciences Center, Vilnius University, Saulėtekio 7, Vilnius LT-10257,  
Lithuania

## Contents

<b>1</b>	<b>On units of length and area</b>	<b>1</b>
<b>2</b>	<b>Default van der Waals radii used by VoroContacts</b>	<b>1</b>
<b>3</b>	<b>Comparing computation of contacts using VoroContacts and dr_sasa software tools</b>	<b>3</b>
3.1	Dataset used for the analysis . . . . .	3
3.2	Comparing contact areas . . . . .	4
3.3	Comparing running times . . . . .	8
3.4	Comparing dependency on the rolling probe radius . . . . .	9
<b>References</b>		<b>11</b>

## 1 On units of length and area

All length values (e.g. radii values) in this document are in angstroms ( $\text{\AA}$ ). All area values — in square angstroms ( $\text{\AA}^2$ ).  $1 \text{\AA} = 10^{-10}$  meters.

## 2 Default van der Waals radii used by VoroContacts

For protein atoms, we use the detailed set published by Li and Nussinov [1], the set is shown in Table S1. For non-protein atoms, we use van der Waals radii values derived from multiple sources. We obtained the radii values for the most common elements in biological macromolecules (Table S2) by averaging and rounding the radii values from the Li and Nussinov set. For elements commonly appearing as ions (Table S3) we used the set of common ionic radii from the CRC Handbook of Chemistry and Physics [2]. For unrecognized atoms the radius value of 1.8 angstroms is assigned.

Table S1: Van der Waals radii used for protein atoms

ALA C	1.75	CYS CB	1.91	HIS NE2	1.6	MET SD	1.94	TRP CA	1.9
ALA CA	1.9	CYS N	1.7	HIS O	1.49	PHE C	1.75	TRP CB	1.91
ALA CB	1.92	CYS O	1.49			PHE CA	1.9	TRP CD1	1.82
ALA N	1.7	CYS SG	1.88	ILE C	1.75	PHE CB	1.91	TRP CD2	1.82
ALA O	1.49			ILE CA	1.9	PHE CD1	1.82	TRP CE2	1.74
		GLN C	1.75	ILE CB	2.01	PHE CD2	1.82	TRP CE3	1.82
ARG C	1.75	GLN CA	1.9	ILE CD1	1.92	PHE CE1	1.82	TRP CG	1.74
ARG CA	1.9	GLN CB	1.91	ILE CG1	1.92	PHE CE2	1.82	TRP CH2	1.82
ARG CB	1.91	GLN CD	1.81	ILE CG2	1.92	PHE CZ	1.82	TRP CZ2	1.82
ARG CD	1.88	GLN CG	1.8	ILE N	1.7	PHE CG	1.74	TRP CZ3	1.82
ARG CG	1.92	GLN N	1.7	ILE O	1.49	PHE N	1.7	TRP N	1.7
ARG CZ	1.8	GLN NE2	1.62			PHE O	1.49	TRP NE1	1.66
ARG N	1.7	GLN O	1.49	LEU C	1.75	PRO C	1.75	TRP O	1.49
ARG NE	1.62	GLN OE1	1.52	LEU CA	1.9	PRO CA	1.9		
ARG NH1	1.62			LEU CB	1.91	PRO CB	1.91	TYR CB	1.91
ARG NH2	1.67	GLU C	1.75	LEU CD1	1.92	PRO CD	1.92	TYR CD1	1.82
ARG O	1.49	GLU CA	1.9	LEU CD2	1.92	PRO CG	1.92	TYR CG	1.74
		GLU CB	1.91	LEU CG	2.01	SER C	1.75	TYR CZ	1.8
ASN C	1.75	GLU CD	1.76	LEU N	1.7	SER CA	1.9	ASN ND2	1.62
ASN CA	1.9	GLU CG	1.88	LEU O	1.49	SER CB	1.9	ASN O	1.49
ASN CB	1.91	GLU N	1.7			SER CD	1.92	ASP OD1	1.52
ASN CG	1.81	GLU O	1.49	LYS C	1.75	THR C	1.75	ASP OD2	1.49
ASN N	1.7	GLU OE1	1.49	LYS CA	1.9	THR CA	1.9	CYS C	1.75
ASN ND2	1.62	GLU OE2	1.49	LYS CB	1.91	THR CB	2.01	CYS CA	1.9
ASN O	1.49			LYS CD	1.92	THR CG2	1.92	ASP C	1.75
ASN OD1	1.52	GLY C	1.75	LYS CE	1.88	THR N	1.7	ASP CB	1.91
		GLY CA	1.9	LYS CG	1.92	SER OG	1.54	ASP CG	1.76
ASP C	1.75	GLY N	1.7	LYS NZ	1.67	SER O	1.49	ASP N	1.7
ASP CA	1.9	GLY O	1.49	LYS O	1.49	THR OG1	1.54	ASP O	1.49
ASP CB	1.91							ASP OD1	1.49
ASP CG	1.76	HIS C	1.75					ASP OD2	1.49
ASP N	1.7	HIS CA	1.9	MET C	1.75			CYS CA	1.9
ASP O	1.49	HIS CB	1.91	MET CA	1.9				
ASP OD1	1.49	HIS CD2	1.74	MET CB	1.91				
ASP OD2	1.49	HIS CE1	1.74	MET CE	1.8				
		HIS CG	1.8	MET CG	1.92				
CYS C	1.75	HIS N	1.7	MET N	1.7				
CYS CA	1.9	HIS ND1	1.6	MET O	1.49				

Table S2: Van der Waals radii used for the most common elements in biological macromolecules

C	1.8	N	1.6	O	1.5	S	1.9	P	1.9
---	-----	---	-----	---	-----	---	-----	---	-----

Table S3: Van der Waals radii used for ions

Al <sup>+3</sup>	0.54	As <sup>+3</sup>	0.58	Au <sup>+1</sup>	1.37	Ba <sup>+2</sup>	1.35	Be <sup>+2</sup>	0.45	Bi <sup>+3</sup>	1.03
Ca <sup>+2</sup>	1.00	Cd <sup>+2</sup>	0.95	Co <sup>+2</sup>	0.65	Cr <sup>+2</sup>	0.73	Cs <sup>+</sup>	1.67	Cu <sup>+2</sup>	0.73
Fe <sup>+2</sup>	0.61	Ga <sup>+3</sup>	0.62	Ge <sup>+2</sup>	0.73	Hg <sup>+2</sup>	1.02	K <sup>+</sup>	1.38	Li <sup>+</sup>	0.76
Mg <sup>+2</sup>	0.72	Mn <sup>+2</sup>	0.83	Mo <sup>+3</sup>	0.69	Na <sup>+</sup>	1.02	Ni <sup>+2</sup>	0.69	Pb <sup>+2</sup>	1.19
Pd <sup>+2</sup>	0.86	Pt <sup>+2</sup>	0.80	Rb <sup>+</sup>	1.52	Sb <sup>+3</sup>	0.76	Sc <sup>+3</sup>	0.75	Sn <sup>+4</sup>	0.69
Sr <sup>+2</sup>	1.18	Tc <sup>+4</sup>	0.65	Ti <sup>+2</sup>	0.86	V <sup>+2</sup>	0.79	Zn <sup>+2</sup>	0.74	Zr <sup>+4</sup>	0.72
F <sup>-</sup>	1.33	Cl <sup>-</sup>	1.81	Br <sup>-</sup>	1.96	I <sup>-</sup>	2.20				

### 3 Comparing computation of contacts using VoroContacts and dr\_sasa software tools

#### 3.1 Dataset used for the analysis

We selected 313 protein chains from PDB using the PISCES server [3]. by applying the following constraints:

- sequence identity between any protein pair is 20% or less;
- X-ray resolution is 1.4 angstroms or better;
- free R-factor is 0.14 or less;
- sequence length is between 50 and 500 residues.

The resulting set of PDB identifiers and chain names is listed in Table S4.

Table S4: Protein structures used for the analysis.

1C5E_A, 1EB6_A, 1G6X_A, 1GCI_A, 1I1W_A, 1IQZ_A, 1IX9_A, 1J0P_A, 1JFB_A, 1K5C_A,
1K7C_A, 1KQP_A, 1KWF_A, 1LWB_A, 1M15_A, 1M4L_A, 1MC2_A, 1MJ5_A, 1MUW_A, 1NKA_A,
1NWZ_A, 1O7J_A, 1OK0_A, 1PSR_A, 1R6J_A, 1SAU_A, 1SFS_A, 1UFY_A, 1US0_A, 1UWC_B,
1VBW_A, 1VYR_A, 1W0N_A, 1W23_A, 1X8Q_A, 1XG0_A, 1XG0_C, 1ZL0_A, 1ZUU_A, 1ZZK_A,
2A3N_A, 2AKZ_A, 2BK9_A, 2BT9_C, 2C71_A, 2CI1_A, 2CNQ_A, 2CS7_A, 2CWS_A, 2FKK_A,
2FVY_A, 2GGC_A, 2GKG_A, 2JFR_A, 2NLR_A, 2NWF_A, 2O7A_A, 2O9S_A, 2OB3_A, 2OFC_A,
2OIZ_A, 2OIZ_D, 2OV0_A, 2PND_A, 2PVB_A, 2R31_A, 2RH2_A, 2UU8_A, 2V3G_A, 2V3I_A,
2V8T_B, 2V9L_A, 2V9V_A, 2VB1_A, 2VXN_A, 2W15_A, 2WFI_A, 2XJP_A, 2XOM_A, 2XTS_A,
2YKZ_A, 2ZK9_X, 3A5F_A, 3A72_A, 3AGN_A, 3D1P_A, 3DLC_A, 3EA6_A, 3EO6_B, 3FSA_A,
3FYM_A, 3G0K_A, 3G21_A, 3G5T_A, 3HWU_A, 3HYN_A, 3IP0_A, 3JQ0_A, 3KWE_A, 3L8W_A,
3LAA_A, 3LWX_A, 3M5Q_A, 3MD7_A, 3MQD_A, 3NVS_A, 3O4P_A, 3PD7_A, 3PPL_A, 3PUC_A,
3Q46_A, 3QHB_A, 3QL9_A, 3QPA_A, 3QR7_A, 3RWN_A, 3S6E_A, 3T2C_A, 3TC8_A, 3TEU_A,
3TG2_A, 3ULJ_A, 3VII_A, 3VOR_A, 3W07_A, 3WDN_A, 3X2M_A, 3X34_A, 3ZOJ_A, 3ZSJ_A,
3ZUC_A, 3ZZP_A, 4A02_A, 4A29_A, 4ACJ_A, 4AFF_A, 4AL0_A, 4AYO_A, 4AZ6_A, 4BJ0_A,
4CE8_C, 4CHI_A, 4CJ0_B, 4CO8_A, 4E3Y_A, 4EIC_A, 4ERC_A, 4F06_A, 4F1V_A, 4FK9_A,
4G9S_B, 4H3U_A, 4HCJ_A, 4HNO_A, 4HS1_A, 4IAU_A, 4JN7_A, 4JXR_A, 4KEF_A, 4KQP_A,
4LF0_A, 4M1X_A, 4M51_A, 4M9V_F, 4MNC_A, 4MTM_A, 4MZC_A, 4N1I_A, 4NDS_A, 4NPD_A,
4O6U_A, 4QEK_A, 4QHW_A, 4QLP_A, 4QLP_B, 4REK_A, 4RXV_A, 4S39_A, 4U9H_S, 4UA6_A,
4UU3_B, 4UYR_A, 4UZG_A, 4W9Z_A, 4WBJ_A, 4WJT_A, 4WKA_A, 4WN5_A, 4WUI_A, 4WWF_A,
4X1Z_B, 4X2R_A, 4X5P_A, 4X9X_A, 4XDX_A, 4Y9W_A, 4YAA_A, 4YI8_A, 4YMY_A, 4ZGF_A,
4ZJU_A, 5A0Y_B, 5A0Y_C, 5A1I_A, 5A71_A, 5A8C_A, 5AGD_B, 5AIG_A, 5AOZ_A, 5CKL_A,
5COF_A, 5CTM_A, 5D8V_A, 5DP2_A, 5DZE_A, 5E9P_A, 5EL9_A, 5EQ7_A, 5EWO_A, 5FBF_A,
5FEW_A, 5GJI_A, 5GTQ_A, 5GV8_A, 5IDB_A, 5IG6_A, 5II6_A, 5IMA_A, 5J4L_A, 5JBX_A,
5JRY_A, 5JUG_A, 5JVI_E, 5L87_A, 5LP9_A, 5LS7_B, 5LS7_D, 5M0W_A, 5M17_A, 5MK9_A,
5MX9_A, 5NFM_A, 5NQO_A, 5NWP_A, 5O2X_A, 5O45_A, 5OHQ_A, 5OL4_A, 5OL4_B, 5OPZ_A,
5SY4_B, 5T5L_A, 5TAB_A, 5TDA_A, 5TIF_A, 5U3A_A, 5W8Q_A, 5WGI_A, 5X9L_A, 5Y0M_A,
5YDE_A, 5Z3E_A, 5ZW7_A, 6A9S_A, 6B8F_A, 6C4Q_A, 6CNW_A, 6DTV_A, 6EF7_A, 6EIO_A,
6EQE_A, 6ER4_B, 6ETL_A, 6EY1_A, 6FM7_A, 6FMC_A, 6GX2_A, 6H10_A, 6H40_A, 6HAV_A,
6HFQ_A, 6I6M_A, 6KFN_A, 6KLZ_A, 6L27_A, 6LL8_A, 6NIB_A, 6NNR_B, 6NP3_A, 6Q00_A,
6QHJ_A, 6RI6_A, 6RK0_A, 6RRV_A, 6RY0_A, 6RYG_A, 6SSD_A, 6TWT_B, 6WQY_A, 6Y4E_A,
6ZEG_B, 6ZEG_C, 7A3H_A, 7A5M_A, 7ADR_A, 7ADR_E, 7ADR_F, 7CN7_C, 7COF_A, 7JJA_A,
7KR0_A, 7JJA_A, 7KR0_A

### 3.2 Comparing contact areas

We processed all the 313 structures with VoroContacts (as a script running Voronota [4]) and dr\_sasa [5] using the same set of van der Waals radii (taken from the dr\_sasa configuration) and the same rolling probe radius of 1.4. As dr\_sasa produces asymmetric contact matrices, we took an average of two dr\_sasa areas for every contact. We compared three categories of contact areas:

- per-atom solvent accessible areas (Figure S1)
- residue-residue contact areas (Figure S2)
- atom-atom contact areas (Figure S3)

The results show that solvent accessible surface areas produced by VoroContacts and dr\_sasa are nearly identical, the residue-residue contact areas are highly correlated (Pearson c.c. = 0.97), and atom-atom contact areas are moderately correlated (Pearson c.c. = 0.83). Analysis of the results showed that oftentimes a contact identified by dr\_sasa was not identified as such by VoroContacts. The reason for such discrepancies is that, to identify contacts, VoroContacts uses the Voronoi tessellation, which takes into account not only the proximity between atoms, but also the structural context. Thus, in the structure tessellation, atoms close by distance may not always be direct neighbors, because of the shielding effect by other neighbors.

Figure S1: Comparison of per-atom solvent accessible areas.

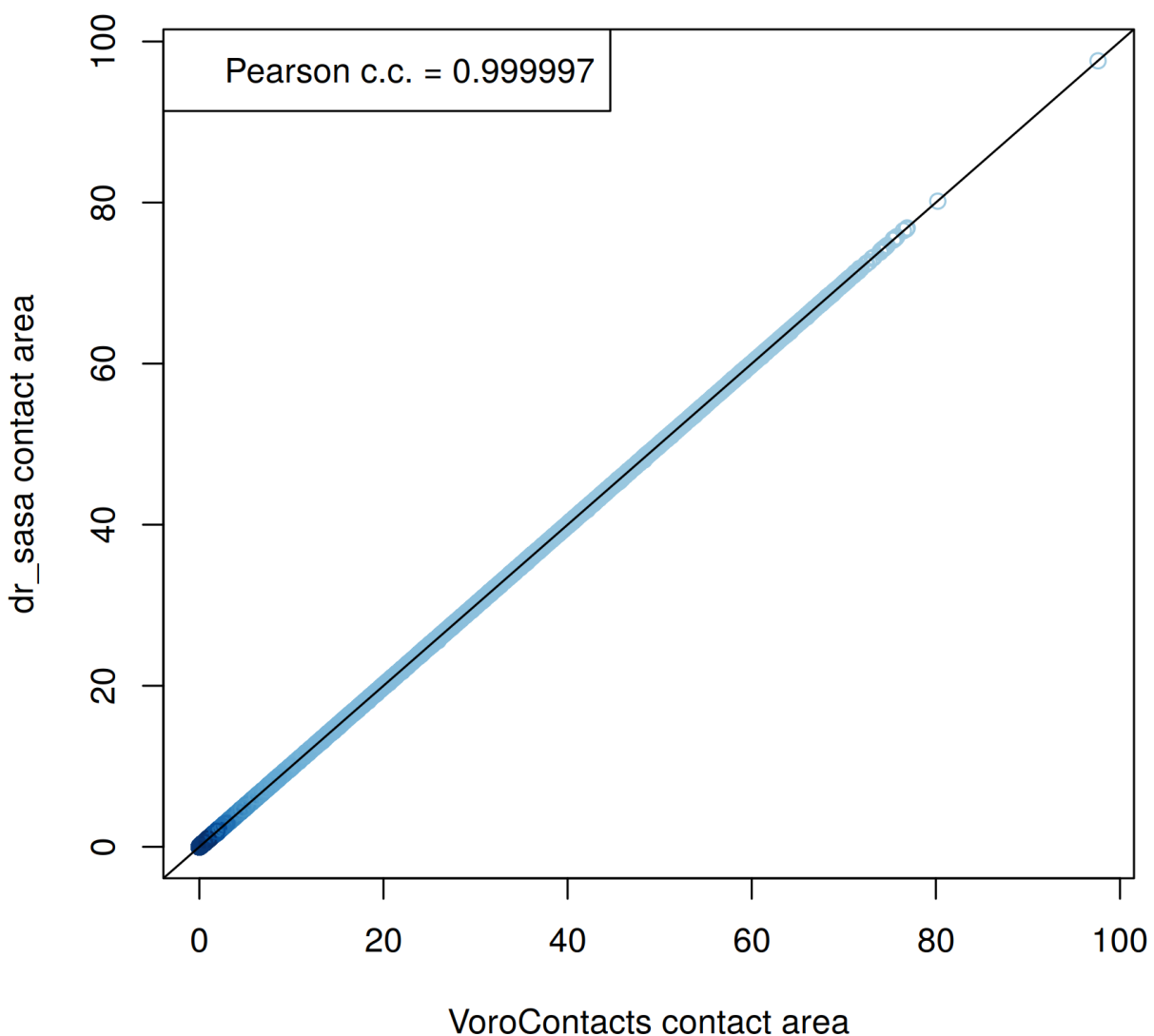


Figure S2: Comparison of residue-residue contact areas.

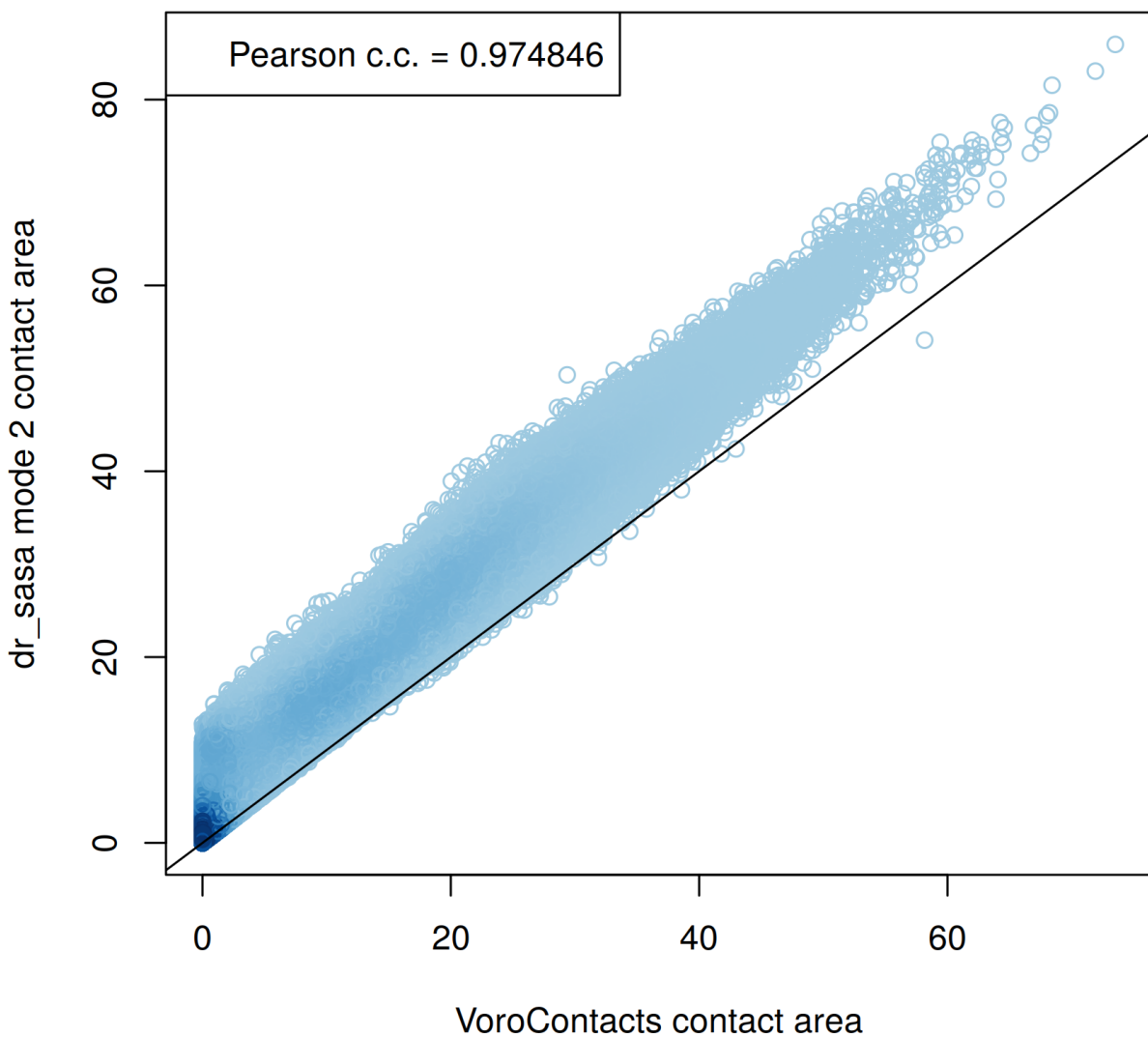
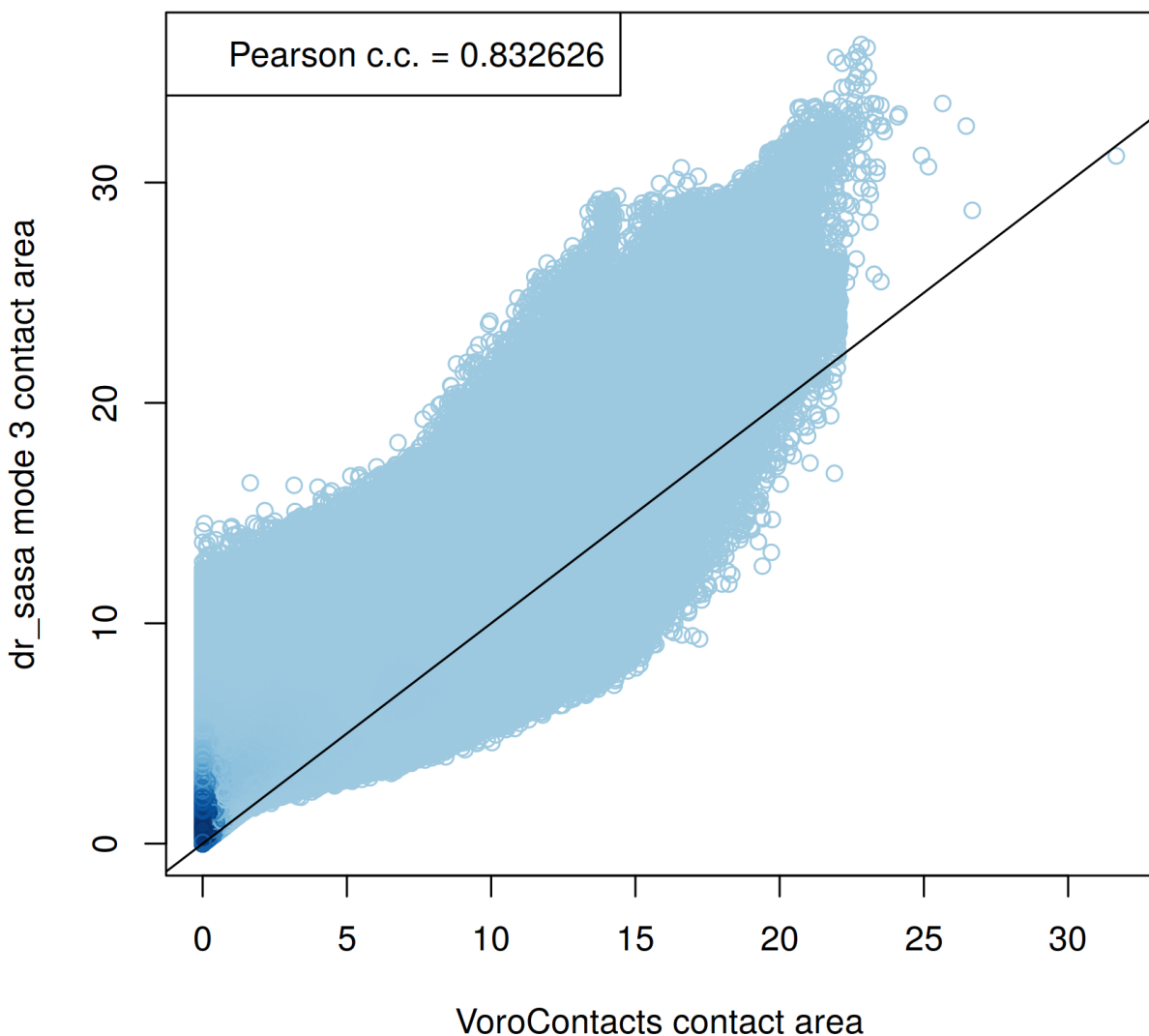


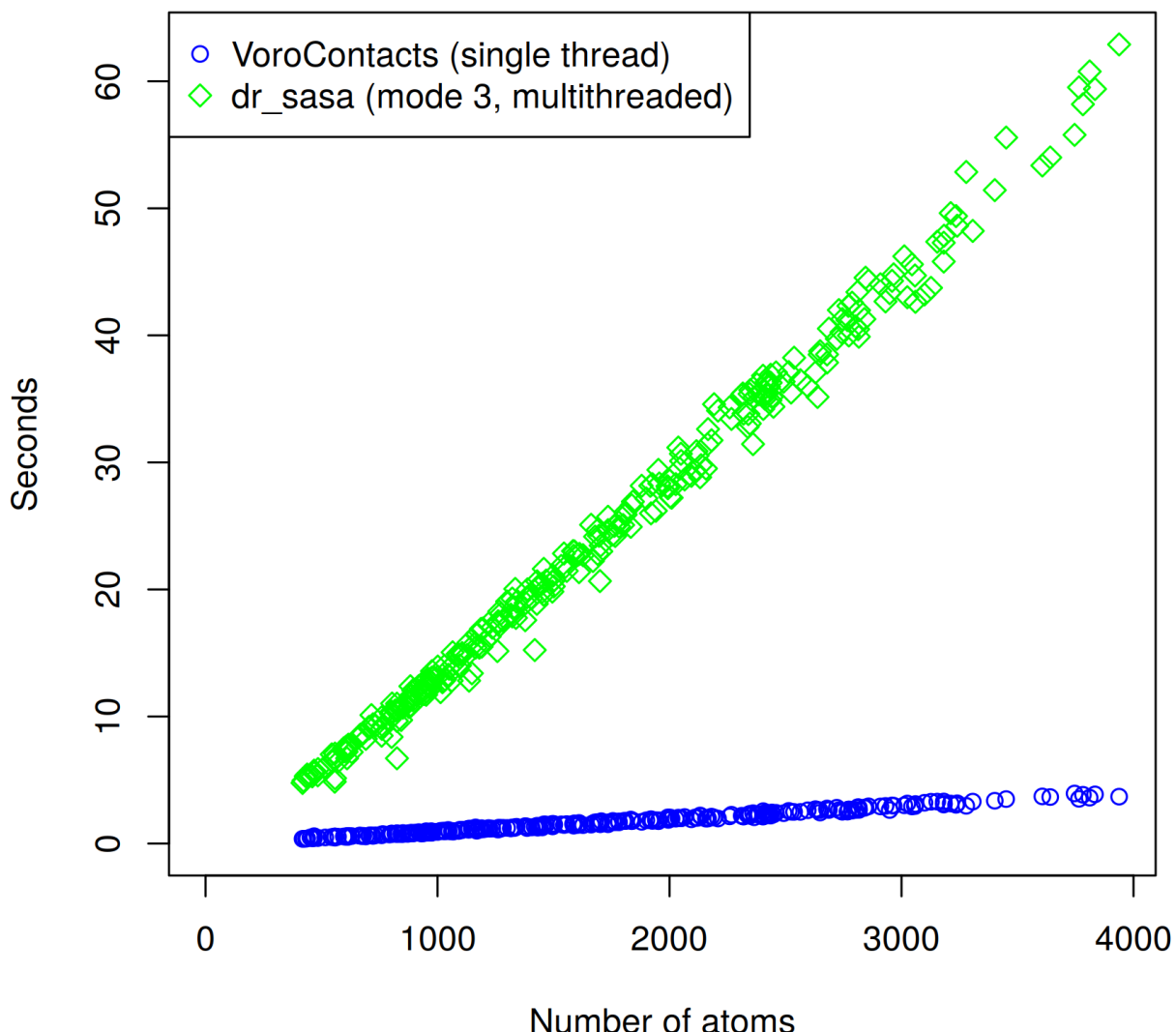
Figure S3: Comparison of atom-atom contact areas.



### 3.3 Comparing running times

We recorded running times on the same machine. Figure S4 shows that VoroContacts was several times faster, despite using only a single thread while dr\_sasa used several.

Figure S4: Comparison of execution times.



### 3.4 Comparing dependency on the rolling probe radius

We investigated how the results of VoroContacts and dr\_sasa depend on the rolling probe radius. We run the software tools on three non-similar protein structures (1C5E\_A, 1EB6\_A, 1G6X\_A) using probe radius parameters ranging from 0.1 to 3.0 angstroms. For every probe radius we counted the number of non-zero-area contacts of the following three categories:

- per-atom solvent accessible surfaces (Figure S5)
- residue-residue contacts (Figure S6)
- atom-atom contacts (Figure S7)

As expected, the numbers of solvent accessible atoms were similar for every probe radius. However, dr\_sasa overestimated the number of residue-residue and atom-atom contacts when executed with larger probe radius parameters. On the other hand, VoroContacts took advantage of the Voronoi tessellation and was much less sensitive to the probe radius increase because it did not consider atoms to be in contact when there are atoms in between them. The performed analysis also suggests that VoroContacts should produce more consistent results when executed using different van der Waals radii.

Figure S5: Number of solvent accessible atoms for various rolling probe radii.

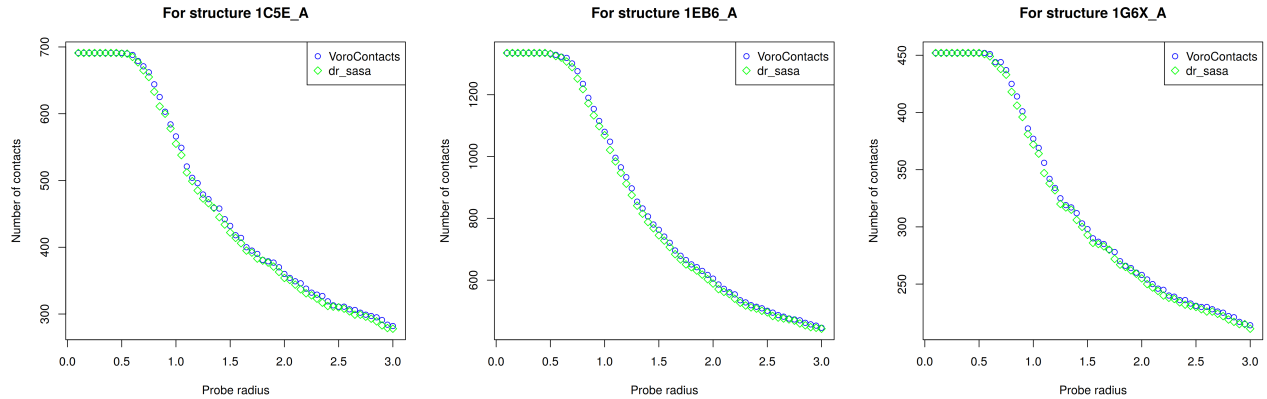


Figure S6: Number of residue-residue contacts for various rolling probe radii.

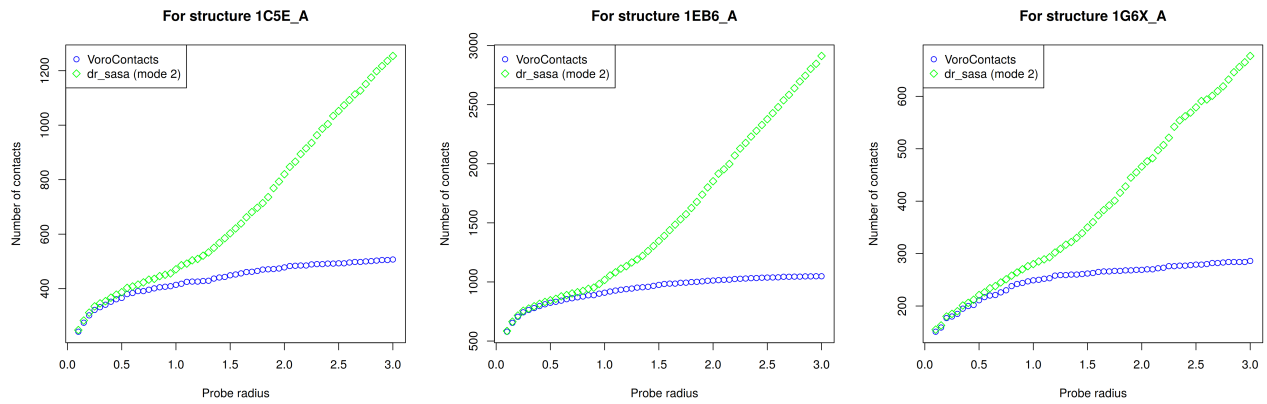
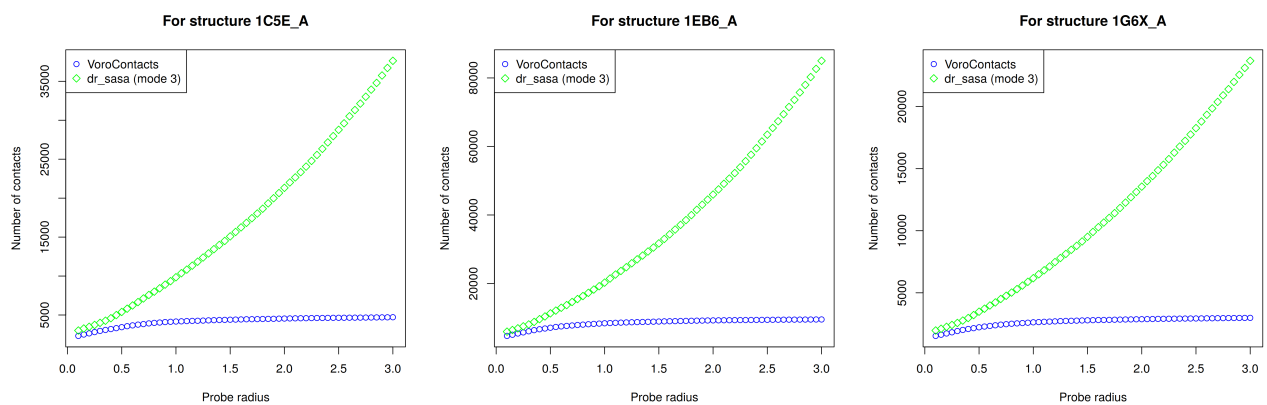


Figure S7: Number of atom-atom contacts for various rolling probe radii.



## References

- [1] A. J. Li and R. Nussinov, "A set of van der Waals and coulombic radii of protein atoms for molecular and solvent-accessible surface calculation, packing evaluation, and docking," *Proteins*, vol. 32, pp. 111–127, July 1998.
- [2] D. R. Lide, ed., *CRC handbook of chemistry and physics: a ready-reference book of chemical and physical data*. Boca Raton: CRC Press, 82. ed., 2001-2002 ed., 2001. OCLC: 248346773.
- [3] G. Wang and R. L. Dunbrack, "PISCES: a protein sequence culling server," *Bioinformatics*, vol. 19, pp. 1589–1591, Aug. 2003.
- [4] K. Olechnovič and C. Venclovas, "Voronota: A fast and reliable tool for computing the vertices of the Voronoi diagram of atomic balls," *J Comput Chem*, vol. 35, pp. 672–681, Mar. 2014.
- [5] J. Ribeiro, C. Ríos-Vera, F. Melo, and A. Schüller, "Calculation of accurate interatomic contact surface areas for the quantitative analysis of non-bonded molecular interactions," *Bioinformatics*, vol. 35, pp. 3499–3501, Sept. 2019.